Tutorial on:
Digital Topology, Geometry and Applications

3rd talk:
3-D simple points, local topological numbers, and applications

Punam Kumar Saha
Professor
Departments of ECE and Radiology
University of Iowa
pksaha@engineering.uiowa.edu

Outline

- Introduction to topological transformation and topological equivalence
- Basic notions of digital topology
- Euler characteristic
- Simple point
- Simple point characterizations in 3-D
- Number of tunnels in $3\times3\times3$ neighborhood
- Local topological numbers
- Efficient algorithms
- Applications

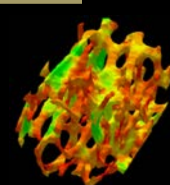

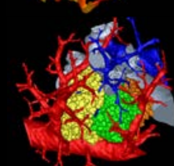

Continuous Deformation

Topology. The study of those properties of geometric figures or solid bodies that remain invariant under certain transformations.

Continuous deformation. A transformation which shrinks, stretches, bents, twists, etc. in any way without tearing

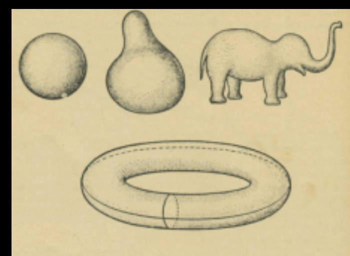

- Envision a figure drawn on a rubber sheet
- A deformation of the sheet by stretching, twisting, bending, etc. which doesn't tear the sheet will change the figure into some other shape

Topological Transformation and Equivalence

Topology. The study of those properties of geometric figures or solid bodies that remain invariant under certain transformations.

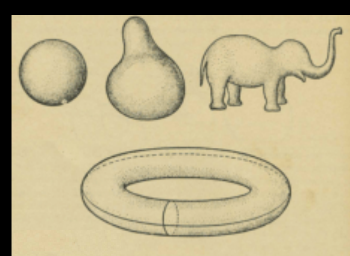

Topological transformation. A transformation that carries one geometric figure into another figure is a topological transformation if the following conditions are met:

1) the transformation is one-to-one
2) the transformation is bicontinuous (i.e. continuous in both directions)

Topologically equivalent. Two different shapes are topologically equivalent if one can be changed to the other by a topological transformation

Basic Definitions in 3-D

- A cubic grid constitutes the set $\mathbb{Z}^3$
- An element of $\mathbb{Z}^3$ is referred to as a point represented by its x-, y-, z-coordinates
- Each cube centered at an element in $\mathbb{Z}^3$ is referred to as a voxel

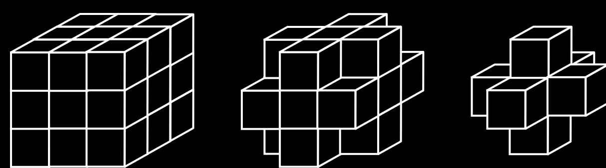

26-adjacency   18-adjacency   6-adjacency

9/16/14   ICPR Tutorial 3rd talk   5

Basic Definitions in 3-D

- An α-path π, where $\alpha \in \{6, 18, 26\}$, is a nonempty sequence $\langle p_0, \cdots, p_{l-1} \rangle$ of voxels where every two successive voxels are α-adjacent

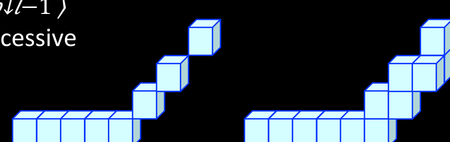

26-path   6-path

- An α-component of a set of voxels S is a maximal subset of S where every two voxels are α-connected in S

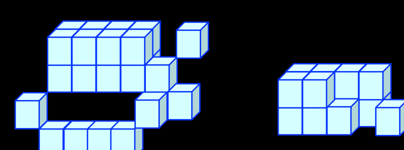

9/16/14   ICPR Tutorial 3rd talk   6

Basic Definitions in 3-D

- An α-path π, where $\alpha \in \{6, 18, 26\}$, is a nonempty sequence $\langle p_0, \cdots, p_{l-1} \rangle$ of voxels where every two successive voxels are α-adjacent

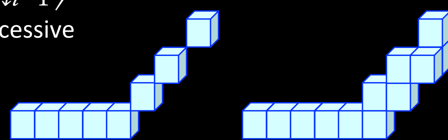

26-path   6-path

- An α-component of a set of voxels S is a maximal subset of S where every two voxels are α-connected in S

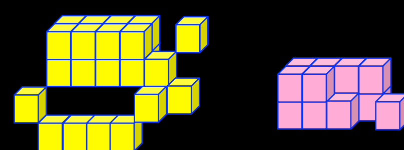

Adjacency Pairs in Digital Topology

- Digital topology loosely refers to the use of mathematical topological properties and features such as connectedness, topology preservation, boundary etc., for images defined in digital grids

Jordan curve

Adjacency Pairs in Digital Topology

- Digital topology loosely refers to the use of mathematical topological properties and features such as connectedness, topology preservation, boundary etc., for images defined in digital grids
- Adjacency pairs. Rosenfeld's approach to digital topology is to use a pair of adjacency relations (κ_1, κ_0) where κ_1 is used for object points while κ_0 is used for background points

Theorem. Jordan curve partitions of a plane into inside and outside

9/16/14 ICPR Tutorial 3rd talk 9

Why the Adjacency Pair?

Rosenfeld convincingly demonstrated that use of a proper adjacency pair leads to workable framework of digital topology, which holds several important mathematical topological properties, including the Jordan curve theorem

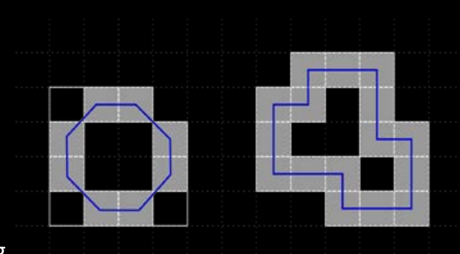

- One proper adjacency pair is (26,6)
- (26,6) is the most popular adjacency pairs in 3-D

The modern trend is to use the cubicial complex representation of digital images to define topological transformation

9/16/14 ICPR Tutorial 3rd talk 10

Cavities and Tunnels in 3-D

- Cavity. A background or white component surrounded by an object component

- Tunnel. Difficult to define a tunnel. However, the number of tunnels in an object is well-defined - the rank of the first homology group of the object.
  - Intuitively, a tunnel would be the opening in the handle of a coffee mug, formed by bending a cylinder to connect the two ends to each other or to another connected object
  - A hollow torus has two tunnels: the first arises from the cavity inside the ring and the second from the ring itself

Euler Characteristic

The Euler characteristic of a polyhedral set X, denoted by $\chi(X)$, is defined as follows

1) $\chi(\phi)=0$
2) $\chi(X)=1$, if X is non-empty and convex
3) for any two polyhedral X, Y, $\chi(X\cup Y)=\chi(X)+\chi(Y)-\chi(X\cap Y)$

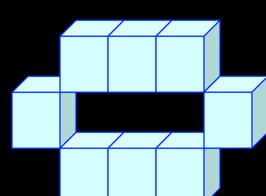

Euler Characteristic: Alternative Definitions

The Euler characteristic of a polyhedron with each element being <u>convex</u>

$$\chi(X) = \#\text{points} - \#\text{edges} + \#\text{faces} - \#\text{volumes},$$

and

$$\chi(X) = \#\text{components} - \#\text{tunnels} + \#\text{cavities}$$

8 – 12 + 6 – 1 = 1

1 – 0 + 0 = 1

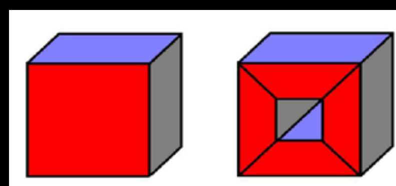

16 – 32 + 20 – 4 = 0

1 – 1 + 0 = 0

3-D Simple Point

Simple Point. A point whose deletion or addition preserves the topology in the local neighborhood in terms of components, tunnels, and cavities

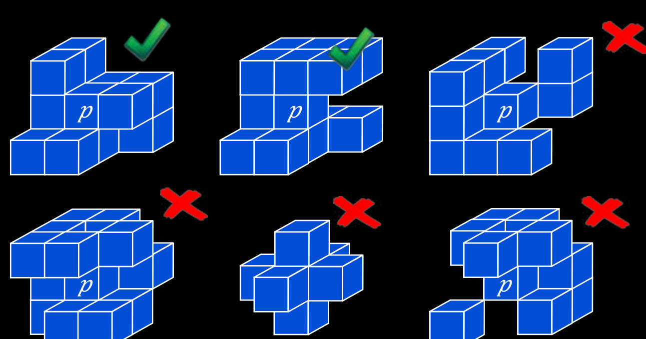

The major challenge. Presence of tunnels in 3-D that is not there in 2-D

3-D Simple Point Characterization by Morgenthaler (1981)

A point $p \in Z^3$ is a (26,6) simple point in a 3-D binary image $(Z^3, 26, 6, B)$ if and only if the following conditions are satisfied

- In $N_{26}^{*}(p)$, the point p is 26-adjacent to exactly one black (object) component
- In $N_{26}^{*}(p)$, the point p is 6-adjacent to exactly one white (background) component
- $\chi((Z^3, 26, 6, (B \cap N(p)) \cup \{p\})) = \chi((Z^3, 26, 6, (B \cap N(p)) - \{p\}))$

$$\boxed{\chi(X) = \#\text{components} - \#\text{tunnels} + \#\text{cavities}}$$

Tunnels on the surface of a Topological Sphere

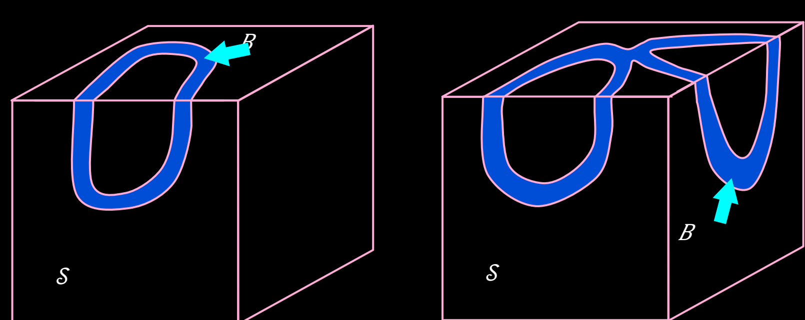

Tunnels on the surface of 3x3x3 neighborhood (Digital Case)

- In a $3{\times}3{\times}3$ neighborhood, if the central voxel is white, all black voxels lie on its outer surface
- For computation of tunnels, a white component must be 6-adjacent to the central voxel
- Ooops still there is some problem!!

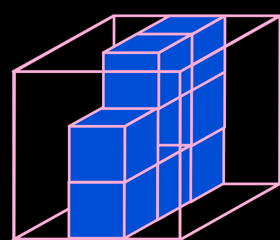

Tunnels on the surface of 3x3x3 neighborhood (Digital Case)

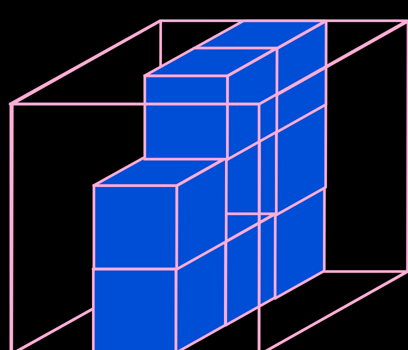

Tunnels on the surface of 3x3x3 neighborhood (Digital Case)

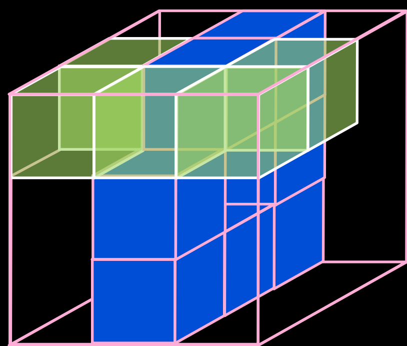

Tunnels on the surface of 3x3x3 neighborhood (Digital Case)

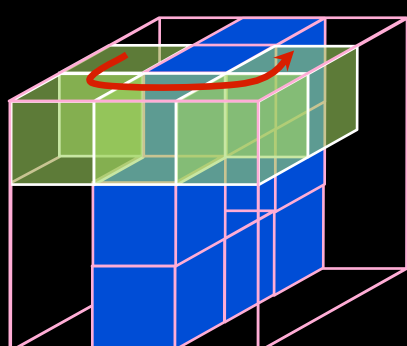

Tunnels on the surface of 3x3x3 neighborhood (Digital Case)

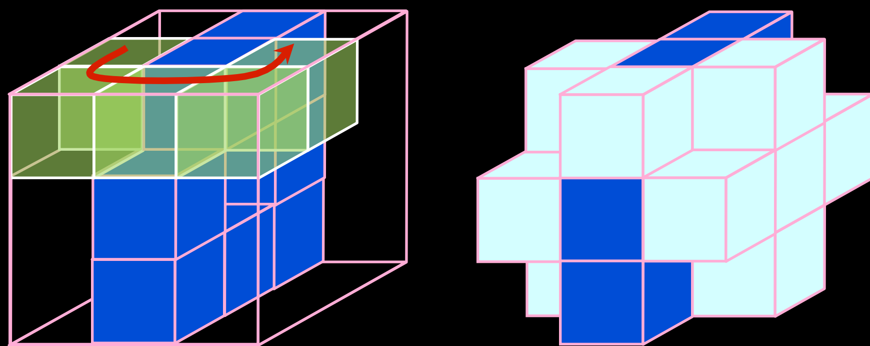

Tunnels on the surface of 3x3x3 neighborhood (Digital Case)

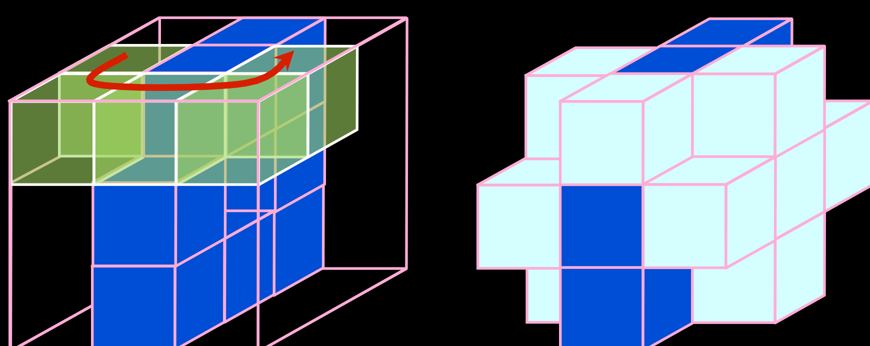

Theorem. If a voxel or point $p \in Z^3$ has at a white 6-neighbor, the number of tunnels $\eta(p)$ in $N_{26}^{*}(p)$ is one less than the number of 6-components of white points in $N_{18}^{*}(p)$ that intersect with $N_{6}^{*}(p)$, or, zero otherwise.

3-D Simple Point Characterization by Saha *et al.* (1991, 1994)

Theorem. If a voxel or point $p \in Z^3$ has at a white 6-neighbor, the number of tunnels $\eta(p)$ in $N_{26}^{*}(p)$ is one less than the number of 6-components of white points in $N_{18}^{*}(p)$ that intersect with $N_{6}^{*}(p)$, or, zero otherwise.

A point $p \in Z^3$ is a (26,6) simple point in a 3-D binary image $(Z^3, 26, 6, B)$ if and only if the following conditions are satisfied

- p has a white (background) 6-neighbor, i.e., $N_{6}^{*}(p) - B \neq \phi$
- p has a black (object) 26-neighbor, i.e., $N_{26}^{*}(p) \cap B \neq \phi$
- The set of black 26-neighbors of p is 26-connected, i.e., $N_{26}^{*}(p) \cap B$ is 26-connected
- The set of white 6-neighbors of p is 6-connected in the set of white 18-neighbors, i.e., $N_{6}^{*}(p) - B$ is 6-connected in $N_{18}^{*}(p) - B$

9/16/14 ICPR Tutorial 3rd talk 23

3-D Simple Point Characterization by Malandain and Bertrand (1992, 1994)

A point $p \in Z^3$ is a (26,6) simple point in a 3-D binary image $(Z^3, 26, 6, B)$ if and only if the following conditions are satisfied

- $N_{26}^{*}(p)$ has exactly one 26-component of black points
- The number of 6-components of white points in $N_{18}^{*}(p)$ that intersect with $N_{6}^{*}(p)$ is exactly one

9/16/14 ICPR Tutorial 3rd talk 24

Local Topological Numbers

- $\xi(p)$: the number of objects components in the 3×3×3 neighborhood after deletion of p
- $\eta(p)$: the number of tunnels in the 3×3×3 neighborhood after deletion of p
- $\delta(p)$: the number of cavities in the 3×3×3 neighborhood after deletion of p

Efficient Computation of 3-D Simple Point and Local Topological Numbers

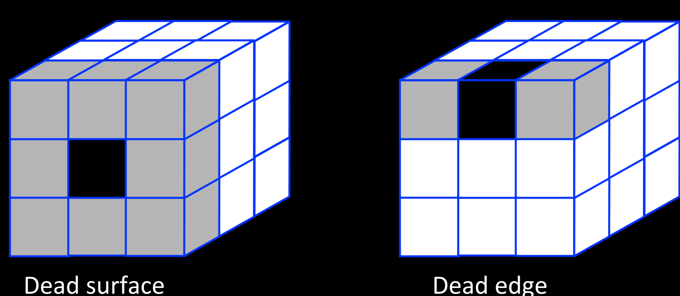

Theorem. 3-D simplicity and local topological numbers of a point is independent of its dead points.

Effective Neighbors

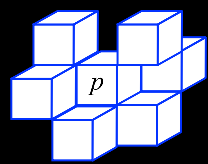

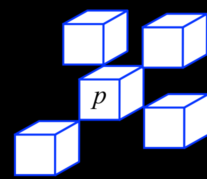

- e (edge)-neighbor: 18-adjacent but not 6-adjacent, i.e., share an edge with p
- Effective e-neighbor: An e-neighbor not belonging to a dead surface

- v (vertex)-neighbor: 26-adjacent but not 18-adjacent, i.e., share a vertex with p
- Effective v-neighbor: A v-neighbor not belonging to a dead surface or a dead edge

Theorem. Object/background configuration 6-neighbors, effective e- and v-neighbors is the necessary and sufficient information to decide on 3-D simplicity and local topological numbers of a point.

Efficient Algorithm

- Determine the object/background configuration of 6-neighbors
- Determine the object/background configuration of effective e-neighbors
- Determine the object/background configuration of effective v-neighbors
- Use look up table to determine 3-D simplicity and the local topological numbers $\xi(p)$, $\eta(p)$, and $\delta(p)$

Topology Preservation in Parallel Skeletonization

The principal challenge in topology preservation for parallel skeletonization

- a characterization of simple point guarantees topology preservation when one simple point is deleted at a time
- however, these characterizations fail to ensure topology preservation when a set of simple points are deleted in parallel

Different Approaches

- Sub-iterative scheme. Divide an iteration into subiterations – (1) based on the direction of open face(s) of boundary voxels or (2) based on subfield partitioning of the image grid
- Minimal non-simple sets. Ronse showed in 2-D that a set of pixels and its proper subsets are all co-deletable if each singleton and each pair of 8-adjacent pixels in the set is co-deletable. This theory leads to topology preservation constraints for parallel skeletonization defined over an extended neighborhood.

Different Approaches

- P-simple points. Bertrand introduced a new interpretation of simple points, referred to a P-simple points, which guarantees topology preservation even when those points are deleted in parallel.
- Critical kernels. It utilizes the following properties of a critical kernel
  - any complex X collapses onto its critical kernel
  - an essential subcomplex $Y \subset X$ includes the critical kernel of $X \Rightarrow X$ collapses onto Y
  - a subcomplex of Y includes the critical kernel of X and Z is an essential subcomplex of X such that $Y \subset Z \Rightarrow Z$ collapses onto Y

Applications

Bone Morphology & Osteoporosis

- Trabecular bone: network of interconnected plates and rods
- Wolff's law (1892): bone grows/ remodels in response to the applied stresses
- Osteoporosis: low bone mineral density and architectural deterioration
- At risk in USA: >40 million
- US health care cost: ~$17B/Y

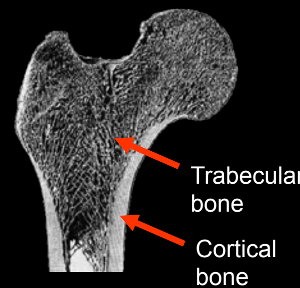

Need improved imaging methods for monitoring bone quality

Bone Mineral Density (BMD) & Architecture

How Predictive is BMD of the Bone's Mechanical Behavior?

- Meta analysis
- N=38 (1985-2000)
- Various parameters of "strength"
- Mean r^2 = 0.64±0.17

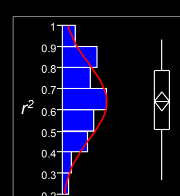

A large number of clinical studies confirm the role of bone architecture to determine bone strength

Quantifying Architecture via Bone Biopsy

- Iliac crest or rib
- Painful, risky, and limited retests
- Not suitable for controls or time-series analysis

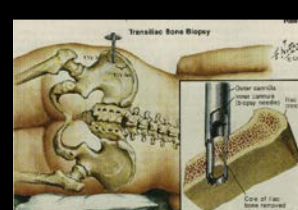

In Vivo Imaging Offers an Opportunity for Virtual Bone Biopsy

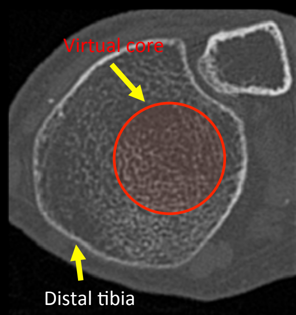

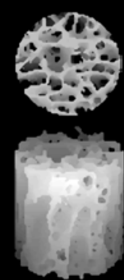

Topology, Scale, Orientation

Features

- Analogous to bone biopsy
- Virtual core is isolated from 3D image data sets.
- Core is subjected to analysis

Challenges

- Reduced resolution
- Limited signal-to-noise ratio

Topology of Trabecular Networks

Topological analysis of line skeletonized structure

3D Euler Poincaré Formula:

χ = objects - tunnels + cavities
= nodes - edges + faces

Connectivity Index = $1-\chi$

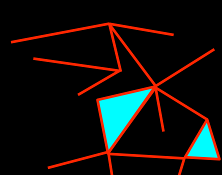

objects: 1
tunnels: 1
cavities: 0

nodes: 17
edges: 19
faces: 2

$\chi=0$

Structure-Model Index (SMI)
SMI μ (∂S/∂r)

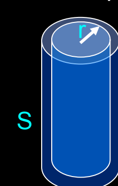

SMI=relative change in surface area (S) upon radial (r) expansion

calcaneus

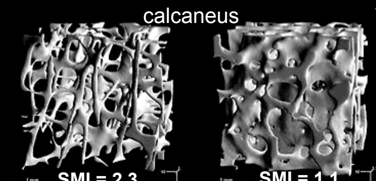

Hildebrand et al, J Bone Miner Res, 1999

Topological Analysis

- Topological class (curve, surface junctions) at any location may be unambiguously determined from the topological numbers (#objects (ξ), #tunnels (η), and #cavities (δ))
- Edge: $\xi = 1$; $\eta = 0$; $\delta = 0$
- Curve Interior: $\xi = 2$; $\eta = 0$; $\delta = 0$
- Surface Interior: $\xi = 1$; $\eta = 1$; $\delta = 0$
- Curve-Curve junction: $\xi > 2$; $\eta = 0$; $\delta = 0$
- Surface-Curve junction: $\xi > 1$; $\eta = 1$; $\delta = 0$
- Surface-Surface junction: $\xi = 1$; $\eta > 1$; $\delta = 0$

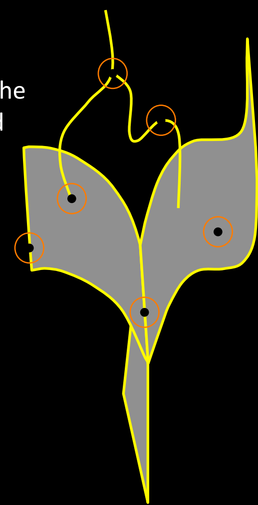

Digital Topological Analysis

- Identifies plates/rods and other topological entities
- Able to distinguish between fracture/ non-fracture groups via *in vivo* MRI
- Being used by several leading research groups

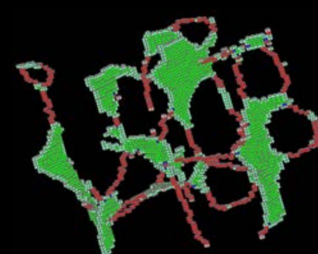

Surface = plate
Rod = curve
Junction

young adult

osteoporotic old age

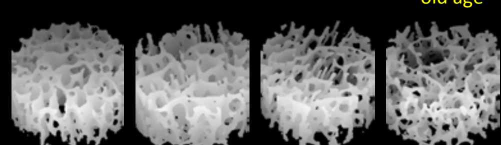

plate-like ←→ rod-like

Surface/Curve(Plate/Rod) Ratio

58.1 15.7 9.8 3.5

Age and disease-related topological changes

Recent Works: Volumetric Topological Analysis

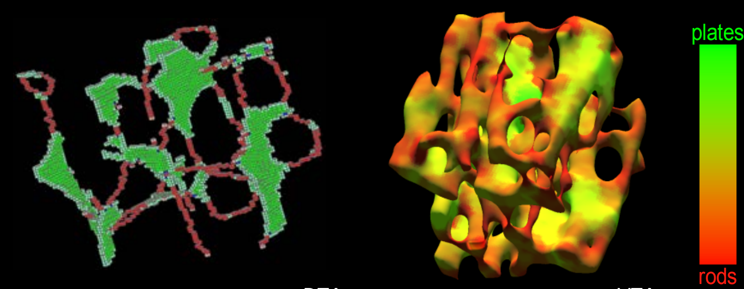

DTA VTA

- Quantify trabecular bone architecture via clinical CT imaging
  - Plateness and rodness on the continuum between perfect plates and perfect rods
  - Local trabecular bone width in the unit of microns

Intermediate Steps

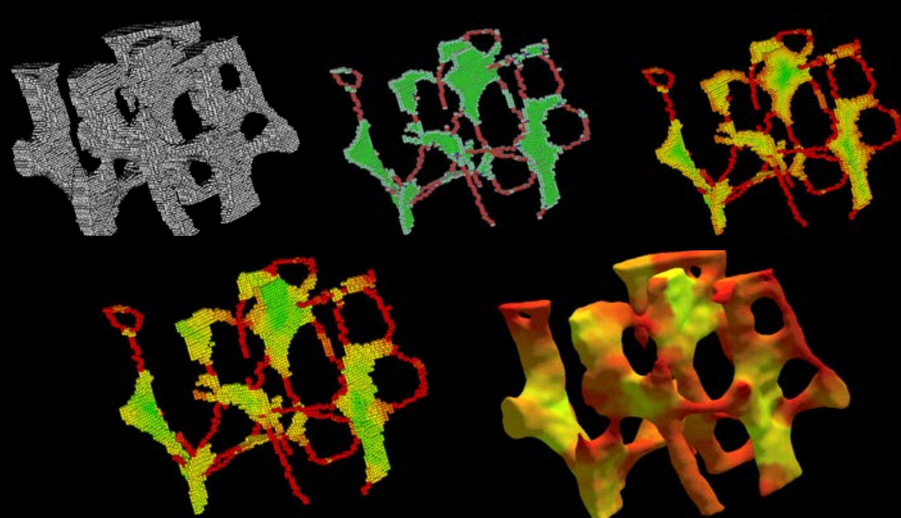

CT Imaging

- 128 slice SOMATOM Definition Siemens Flash scanner
- 120 kV, 200 mAs, pitch: 1.0
- nominal collimation: 16x0.3mm
- scan length: 10 cm
- slice thickness: 300 μm

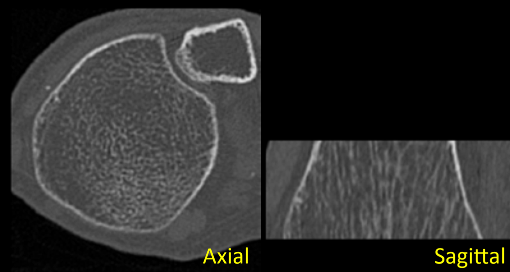

High Intra- and Inter-Modality Reproducibility

Three repeat CT scans

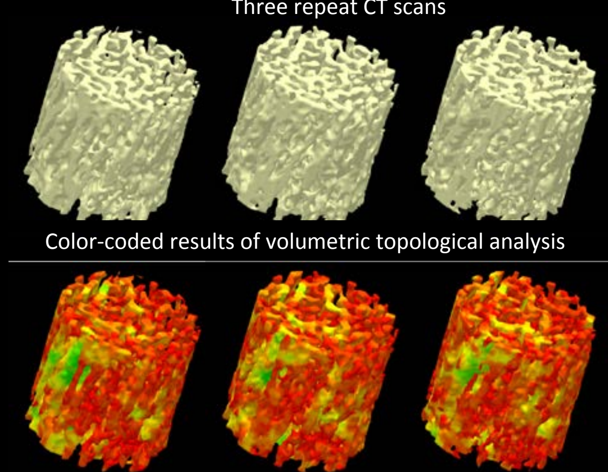

Repeat CT scan
ICC: 0.97

VTA Measure for TB with Distinctively Different Strengths

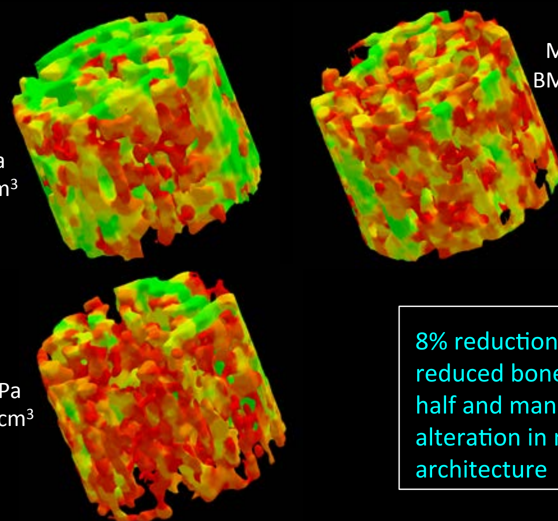

Modulus: 2.2 GPa
BMD: 1.27 gm/cm^3
SW_{VTA}: 385 µm
SCR_{VTA}: 0.38

Modulus: 3.3 GPa
BMD: 1.31 gm/cm^3
SW_{VTA}: 464 µm
SCR_{VTA}: 0.58

Modulus: 1.5 GPa
BMD: 1.20 gm/cm^3
SW_{VTA}: 340 µm
SCR_{VTA}: 0.26

8% reduction in BMD reduced bone strength to half and manifest a 50% alteration in micro-architecture

Ability To Predict Mechanical Properties

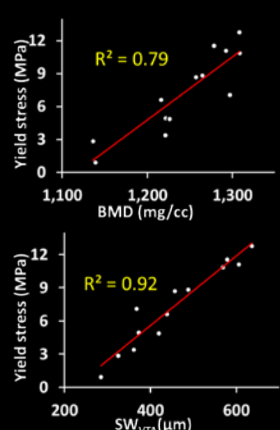

High predictability of experimental biomechanical properties.

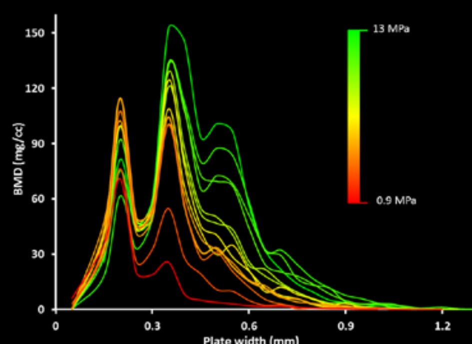

Bone mass distribution at different plate width: a new class of information

Bone Characterization in Different Human Groups

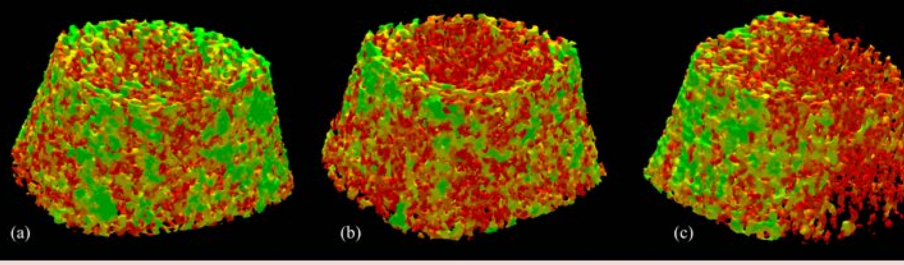

Color-coded illustration of trabecular bone (TB) plate/rod classification for a IBDS female control (a) and an age-similar, sex- and BMI-matched patient on continuous treatment with an SSRI (b), and another age-similar, sex- and BMI-matched patient with confirmed diagnosis of CF (c). The healthy female (a) has more TB plates (green) as compared to the two patient participants. Between the two patients, the CF patient (c) has some signs of heterogeneous bone loss.

Bone Micro-Architecture among Eugonadal and Hypogonadal Men

N = 20 MRI Study

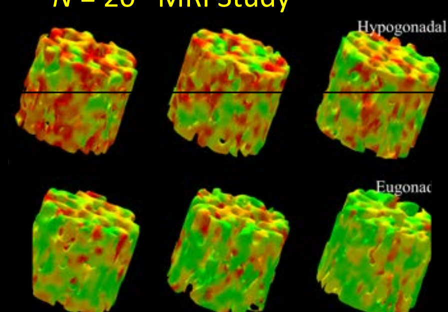

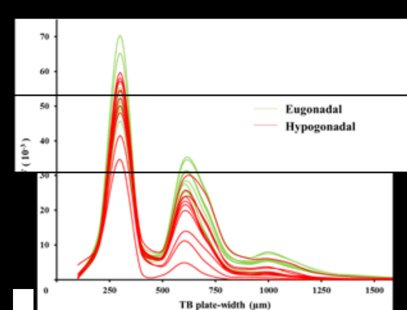

Trabecular bone plate-rod micro-architecture among hypogonadal and eugonadal men

Bone mass distribution at different plate width: a new class of information

- 44 % (p = 0.001) reduction in trabecular bone plate volume
- No significant difference in rod volume

Treatment Effects Hypogonadal Men

N = 10 Two year follow-up MRI study

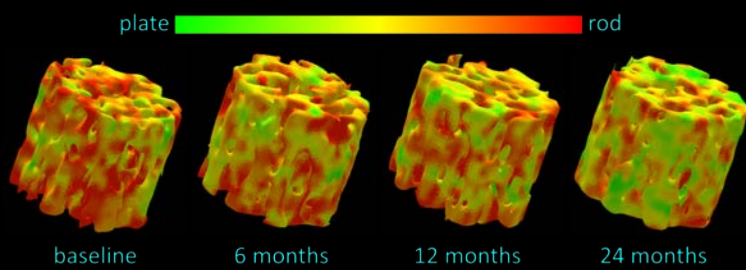

Treatment effects in trabecular bone plate-rod micro-architecture in hypogonadal men

- 6.5 % (p = 0.06) increase in trabecular bone plate volume after 6 months
- 16.2 % (p = 0.003) increase in trabecular bone plate volume after 24 months
- No significant difference in rod volume even after 24 months of treatment

Questions ?

Thank You

Conclusion

- The issues of sequential topological transformation in 3-D cubic grid (3-D simple point) are well-addressed in literature
- Local topological properties are useful to characterize 1-D and 2-D digital manifolds and their junctions
- Different approaches have been should for topology preservation in parallel skeletonization
- Local neighborhood topology is useful in medical imaging applications

References

1. A. Rosenfeld, "Digital topology," *American Mathematical Monthly,* vol. 86, pp. 621-630, 1979.
2. A. Rosenfeld, "Adjacency in digital pictures," *Information and Control,* vol. 26, pp. 24-33, 1974.
3. T. C. Hales, "The Jordan curve theorem, formally and informally," *The American Mathematical Monthly,* pp. 882-894, 2007.
4. T. Kong and A. Roscoe, "Continuous analogs of axiomatized digital surfaces," *Computer Vision, Graphics, and Image Processing,* vol. 29, pp. 60-86, 1985.
5. T. Y. Kong and A. W. Roscoe, "A theory of binary digital pictures," *Computer Vision, Graphics, and Image Processing,* vol. 32, pp. 221-243, 1985.
6. E. D. Khalimsky, "Topological structures in computer science," *Journal of applied mathematics and simulation,* vol. 1, pp. 25-40, 1987.
7. V. A. Kovalevsky, "Finite topology as applied to image processing," *Computer Vision Graphics and Image Processing,* vol. 46, pp. 141-161, 1989.
8. T. Y. Kong and A. Rosenfeld, "Digital topology: introduction and survey," *Computer Vision, Graphics, and Image Processing,* vol. 48, pp. 357-393, 1989.
9. R. Klette and A. Rosenfeld, *Digital Geometry: Geometric Methods for Digital Picture Analysis*. Morgan Kaufmann, San Francisco, CA, 2004.
10. T. Y. Kong and A. Rosenfeld, *Topological algorithms for digital image processing*. Elsevier, 1996.
11. K. Voss, "Images, objects, and surfaces in Zn," *International journal of pattern recognition and artificial intelligence,* vol. 5, pp. 797-808, 1991.

References

12. P. K. Saha and B. B. Chaudhuri, "A new approach of computing Euler characteristic," *Pattern Recognition,* vol. 28, pp. 1955-1963, 1995.
13. T. Y. Kong, A. W. Roscoe, and A. Rosenfeld, "Concepts of digital topology," *Topology and its Applications,* vol. 46, pp. 219-262, 1992.
14. G. Tourlakis and J. Mylopoulos, "Some results on computational topology," *J. Assoc. Comput. Mach.,* vol. 20, pp. 439-455, 1973.
15. D. G. Morgenthaler, "Three-dimensional simple points: serial erosion, parallel thinning and skeletonization," Computer Vision Laboratory, University of Maryland, College Park, MD, 1981.
16. S. Lobregt, P. W. Verbeek, and F. C. A. Groen, "Three-dimensional skeletonization, principle, and algorithm," *IEEE Trans. Pattern Analysis Mach. Intell.,* vol. 2, pp. 75-77, 1980.
17. P. K. Saha, B. B. Chaudhuri, B. Chanda, and D. D. Majumder, "Topology preservation in 3D digital space," *Pattern Recognition,* vol. 27, pp. 295-300, 1994.
18. P. K. Saha, B. Chanda, and D. D. Majumder, "Principles and algorithms for 2-D and 3-D shrinking," Indian Statistical Institute, Calcutta, India, TR/KBCS/2/91, 1991.
19. P. K. Saha and B. B. Chaudhuri, "Detection of 3-D simple points for topology preserving transformations with application to thinning," *IEEE Transactions on Pattern Analysis and Machine Intelligence,* vol. 16, pp. 1028-1032, 1994.
20. P. K. Saha, "2D thinning algorithms and 3D shrinking," INRIA, Sophia Antipolis Cedex, France, June, 1991.

References

21. G. Malandain and G. Bertrand, "Fast characterization of 3-D simple points," *Proceedings of the 11th International Conference on Pattern Recognition*, pp. 232-235, 1992.
22. G. Bertrand and G. Malandain, "A new characterization of three-dimensional simple points," *Pattern Recognition Letters,* vol. 15, pp. 169-175, 1994.
23. P. K. Saha and A. Rosenfeld, "Determining simplicity and computing topological change in strongly normal partial tilings of R^2 or R^3," *Pattern Recognition,* vol. 33, pp. 105-118, 2000.
24. P. K. Saha and B. B. Chaudhuri, "3D digital topology under binary transformation with applications," *Computer Vision and Image Understanding,* vol. 63, pp. 418-429, 1996.
25. A. Huang, H. M. Liu, C. W. Lee, C. Y. Yang, and Y. M. Tsang, "On concise 3-D simple point characterizations: a marching cubes paradigm," *IEEE Trans Med Imaging,* vol. 28, pp. 43-51, 2009.
26. S. Fourey and R. Malgouyres, "A concise characterization of 3D simple points," *Discrete Applied Mathematics,* vol. 125, pp. 59-80, 2003.
27. G. Bertrand, "Simple points, topological numbers and geodesic neighborhoods in cubic grids," *Pattern Recognition Letters,* vol. 15, pp. 1003-1011, 1994.
28. T. Y. Kong, "A digital fundamental group," *Computers & Graphics,* vol. 13, pp. 159-166, 1989.
29. G. Borgefors, I. Nyström, and G. S. d. Baja, "Connected components in 3D neighbourhoods," *Proceedings of the Scandinavian conference on image analysis*, pp. 567-572, 1997.

References

30. T. Y. Kong, "Topology-preserving deletion of 1's from 2-, 3-and 4-dimensional binary images," *Proceedings of the International Workshop on Discrete Geometry for Computer Imagery*, Montpellier, France, pp. 1-18, Springer, 1997.
31. P. J. Giblin, *Graphs, surfaces and homology*. Cambridge University Press Cambridge, 2010.
32. M. Couprie and G. Bertrand, "New characterizations of simple points in 2D, 3D, and 4D discrete spaces," *IEEE Transactions on Pattern Analysis and Machine Intelligence,* vol. 31, pp. 637-648, 2009.
33. G. Bertrand, "On P-simple points," *Comptes Rendus de l'Académie des Sciences de Paris (Computer Science/Theory of Signals), Série Math.,* vol. 1, 321, pp. 1077-1084, 1995.
34. G. Bertrand, "P-simple points: A solution for parallel thinning," *Proceedings of the 5th Conf. on Discrete Geometry*, France, pp. 233-242, 1995.
35. G. Malandain, G. Bertrand, and N. Ayache, "Topological segmentation of discrete surfaces," *International Journal of Computer Vision,* vol. 10, pp. 183-197, 1993.
36. S. Svensson, I. Nyström, and G. S. d. Baja, "Curve skeletonization of surface-like objects in 3d images guided by voxel classification," *Pattern Recognition Letters,* vol. 23, pp. 1419-1426, 2002.
37. L. Serino, G. S. d. Baja, and C. Arcelli, "Using the skeleton for 3D object decomposition," *Proceedings of the Scandinavian Conference on Image Analysis*, A. Heyden and F. Kahl (Eds.), Ystad Saltsjöbad, Sweden, vol. LNCS 6688, pp. 447-456, Springer 2011.
38. B. G. Gomberg, P. K. Saha, H. K. Song, S. N. Hwang, and F. W. Wehrli, "Topological analysis of trabecular bone MR images," *IEEE Transactions on Medical Imaging,* vol. 19, pp. 166-174, 2000.

References

39. P. K. Saha, B. R. Gomberg, and F. W. Wehrli, "Three-dimensional digital topological characterization of cancellous bone architecture," *International Journal of Imaging Systems and Technology,* vol. 11, pp. 81-90, 2000.
40. F. W. Wehrli, B. R. Gomberg, P. K. Saha, H. K. Song, S. N. Hwang, and P. J. Snyder, "Digital topological analysis of in vivo magnetic resonance microimages of trabecular bone reveals structural implications of osteoporosis," *Journal of Bone Mineral Research,* vol. 16, pp. 1520-31, 2001.
41. G. Chang, S. K. Pakin, M. E. Schweitzer, P. K. Saha, and R. R. Regatte, "Adaptations in trabecular bone microarchitecture in Olympic athletes determined by 7T MRI," *J Magn Reson Imaging,* vol. 27, pp. 1089-95, 2008.
42. G. A. Ladinsky, B. Vasilic, A. M. Popescu, M. Wald, B. S. Zemel, P. J. Snyder, L. Loh, H. K. Song, P. K. Saha, A. C. Wright, and F. W. Wehrli, "Trabecular structure quantified with the MRI-based virtual bone biopsy in postmenopausal women contributes to vertebral deformity burden independent of areal vertebral BMD," *J Bone Miner Res,* vol. 23, pp. 64-74, 2008.
43. X. S. Liu, P. Sajda, P. K. Saha, F. W. Wehrli, G. Bevill, T. M. Keaveny, and X. E. Guo, "Complete volumetric decomposition of individual trabecular plates and rods and its morphological correlations with anisotropic elastic moduli in human trabecular bone," *J Bone Miner Res,* vol. 23, pp. 223-35, 2008.
44. M. Stauber and R. Muller, "Volumetric spatial decomposition of trabecular bone into rods and plates--a new method for local bone morphometry," *Bone,* vol. 38, pp. 475-84, 2006.

References

45. P. K. Saha, Y. Xu, H. Duan, A. Heiner, and G. Liang, "Volumetric topological analysis: a novel approach for trabecular bone classification on the continuum between plates and rods," *IEEE Trans Med Imaging,* vol. 29, pp. 1821-1838, 2010.